Electronic Supporting Information

Boosting photocatalytic H_2 evolution activity of CdS/N-doped $ZnIn_2S_4$ direct Z-scheme heterostructure by band alignment regulation strategy

Xiaoyan Cai,[a,b] Miao Su,[a] Zhongtian Zeng,[a] Haifeng Weng,[a] Zhiguo Cai,[a] Junying Zhang,[c] Liang Mao*[,a,b]

[a] *School of Materials Science and Physics, China University of Mining and Technology, Xuzhou 221116, China*

[b] *Jiangsu Province Engineering Laboratory of High Efficient Energy Storage Technology and Equipment, China University of Mining and Technology, Xuzhou 221116, China*

[c] *School of Physics, Beihang University, Beijing 100191, China*

*Corresponding author. E-mail: maoliang@cumt.edu.cn

Experimental Section

Preparation of N-doped $ZnIn_2S_4$

The diagrammatic sketch of the sample preparation route is displayed in **Scheme S1**. Firstly, N-doped $ZnIn_2S_4$ (N-ZIS) was prepared by a facile hydrothermal treatment. 0.4 mmol $Zn(CH_3COO)_2 \cdot 2H_2O$, 0.8 mmol $InCl_3$ and 1.6 mmol thioacetamide were dissolved in 18 mL deionized water. Then 12 mL of N,N-dimethylformamide (DMF) was added. After stirring for 30 min, the solution was transferred into a 50 ml Teflon-lined autoclave and kept at 180 °C for 24 h. Afterward, the product was obtained by washing with ethanol several times and drying at 60 ˚C in vacuum. Pure ZIS was synthesized under the same condition except the addition of DMF.

Preparation of CdS/N-doped $ZnIn_2S_4$

Afterwards, CdS nanoparticles were *in-situ* deposited on the surface of N-ZIS using a chemical bath deposition. Typically, 1 M ammonia solution, 1 mM $CdSO_4$ and 5 mM thiourea were firstly dissolved. The N-ZIS sample was then dispersed in the CdS precursor solution under a water bath of 60 ˚C. After stirring for 10 min, the CdS decorated N-ZIS nanostructures were washed with deionized water and then dried at 60 ˚C in vacuum. Energy dispersive X-ray spectrum (EDS) was used to analyze the content of CdS precipitation on N-ZIS surface, and the CdS precursors were accordingly adjusted to obtain a series of composites with different CdS content. The obtained samples were denoted as 0.05CdS/N-ZIS, 0.1CdS/N-ZIS, and 0.15CdS/N-ZIS, respectively, where the prefixes indicated the theoretical weight percentage of CdS in the CdS/N-ZIS hybrids. Typically, the material used for characterizations and

photocatalytic tests was the 0.1CdS/N-ZIS sample (CdS/N-ZIS for clarity) unless otherwise stated. Bare CdS nanoparticles were prepared under the same condition without the addition of $ZnIn_2S_4$.

Photocatalytic H_2 production

Hydrogen evolution measurements were performed by dispersing 10 mg of the photocatalysts powders into 15 mL of aqueous solution containing Na_2S (0.35 M) and Na_2SO_3 (0.25 M), and stirred for 30 min to ensure homogeneity. In order to remove the dissolved oxygen, the mixed solution used in the photocatalytic experiment was bubbled with pure nitrogen for 20 min prior to each test. Under constant magnetic stirring, the system was exposed under visible light and simulated solar light by using Xenon lamp (Perfect Light, China; 500 mW cm^{-2}) with a cut-off filter ($\lambda > 400$ nm), respectively. The reaction solution was stirred constantly during the whole photocatalysis process at room temperature. The evolved H_2 amount was analyzed using a gas chromatographer (Shimadzu GC-2030) equipped with a thermal conductivity detector and the high-purity nitrogen as carrier gas. The apparent quantum efficiency (AQE) of the hydrogen evolution was estimated using the following equation:

$$\mathrm{AQE} = \frac{Number\ of\ evolved\ H_2 \times 2}{Number\ of\ incident\ photons} \times 100\%$$

Materials characterization

The crystal phase of the samples was analyzed by XRD (Bruker D/max-V2500) with a Cu Kα radiation (λ=1.54056 Å) source. The morphology of the samples was characterized by FESEM (Hitachi SU8220) and TEM (Tecnai G2 F20). The

composition of the samples was analyzed using an energy dispersive EDS which was equipped to FESEM. XPS performing on Thermo Fisher K-Alpha was used to analyze the chemical composition of the samples. UV-vis diffuse reflectance spectroscopy was obtained through a VARIAN Cary300 Conc ultraviolet-visible near-infrared spectrometer equipped. The PL spectrum was collected by the FLS980 fluorescence spectrometer. To measure the PL lifetime, the excitation wavelength (λ_{ex}) used was 405 nm and the maximum emission wavelength (λ_{em}) was 560 nm. The average life (Ave. τ) was calculated based on $\tau = \tau_1 * a_1 + \tau_2 * a_2$ (τ_i is the lifetime; a_i is the relative strength). EPR was performed on JEOL-FA 200 spectrometer with a modulation frequency of 100 kHz and a microwave power of 15 mW.

Photoelectrochemical measurements

The photocurrent *vs.* time (I-t), electrochemical impedance spectroscopy (EIS) and Mott-Schottky (M-S) plots were collected by a typical three-electrode system connected with a CHI-660E electrochemical workstation (ChenHua Instrument Co. Ltd.). A typical three-electrode system includes a working electrode, a reference electrode of saturated calomel electrode (SCE), and a counter electrode of Pt wire. Xenon lamp is utilized as the irradiation source in the photoelectrochemical measurements with an intensity of 100 mW cm^{-2}. Transient photocurrent measurements were conducted in a 0.5 M Na_2SO_4 solution, light at first, then dark for 10s at intervals. The working electrode was prepared as follows: 10 mg of catalyst was dispersed in 40 μL of ethanol aqueous solution (H_2O:CH_3OH=1:1) and then mixed with 10 μL 5% Nafion solution by sonicating for 20 min. Finally, 10 μL of the abovementioned

suspension was deposited on the FTO (1×2 cm^2) and dried at room temperature.

Computational method

All calculations are performed with the comemmerial vasp code. which spans reciprocal space with a plane-wave basis and uses the projector-augmented wave (PAW) method. The generalized-gradient approximation (GGA) with the exchange-correlation functional of Perdew-Burke-Ernzerhof (PBE) is employed as the exchange-correlation [S1, 2]. For the plane-wave basis set, a cutoff of E_{cut} = 500 eV, energy convergence of 1×10^{-4} eV, forced convergence of 0.01 eV/Å have been used. A 2×2×1 supercell include 56 atoms is used for the calculation of formation of N doping. The Monkhorst–Pack k-point mesh is 3×3×1. To determine the favorable atomic substitutional form of N in ZIS, the formation energy E_s for defected structure is calculated as follows: $E_f = E_{N-ZIS} + \mu_S - (E_{ZIS} + \mu_N)$, where E_{ZIS} and $E_{N\text{-}ZIS}$ are the energies for pristine ZIS and structure with defects, respectively. The chemical potential of S and N atom are derived from the elementary substance.

The slab model is used for surface computations. A vacuum of approximately 15 Å is placed above the slabs to separate the interaction between periodic images. For N-$ZnIn_2S_4$ (001) surface slab model, a 2×2 single atomic layer including 1 N atom, 31 S atoms, 8 Zn atoms and 16 In atoms is used. For CdS (111) surface slab model, a 2×2 6 atomic layers is used. The k-point grid is 3×3×1.

Supplementary results and discussion

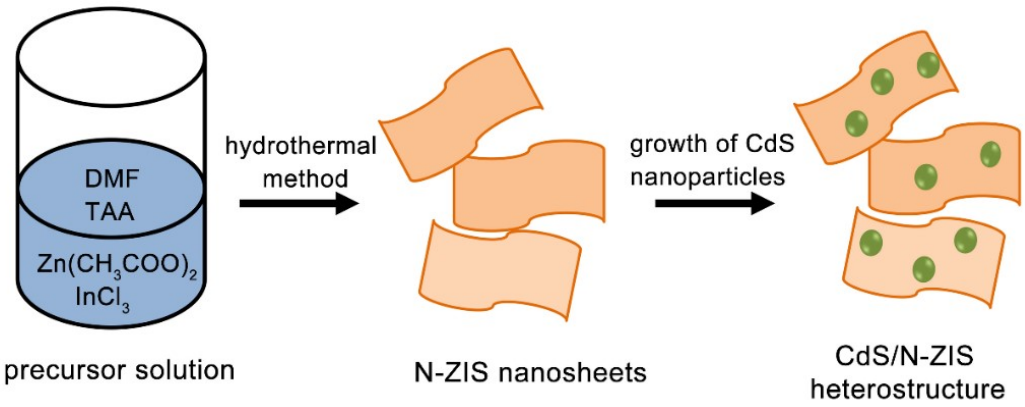

Scheme S1. Diagrammatic sketch of the preparation route of CdS/N-ZIS heterostructure.

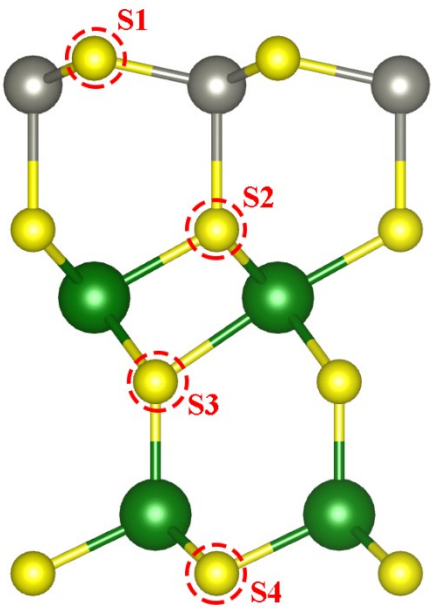

Fig. S1 Crystal structure and N substitution sites of ZIS. The gray, green and yellow balls represent for Zn, In, and S atoms, respectively.

Table S1. Formation energy of the different N substituted forms in Fig. S1.

Sites	S1	S2	S3	S4
E_f (eV)	-2.7902	-4.1416	-4.5461	-4.8146

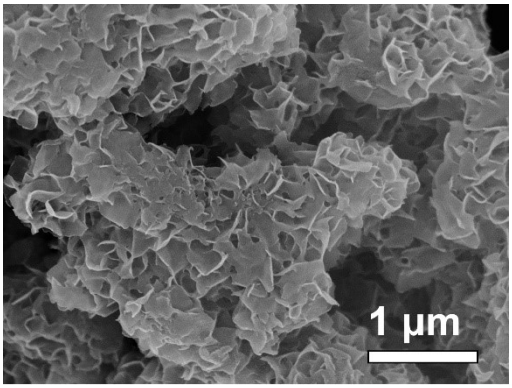

Fig. S2 SEM images of ZIS.

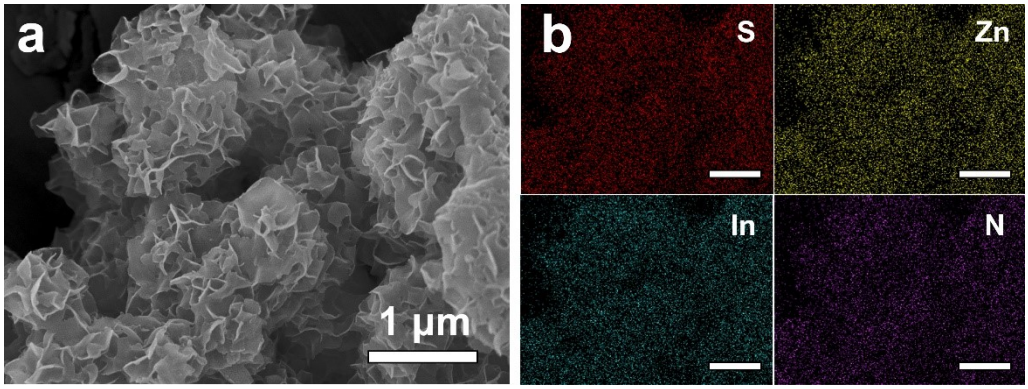

Fig. S3 SEM images of N-ZIS (a), EDS elemental mapping of N-ZIS (b), the scale bars are 1 μm.

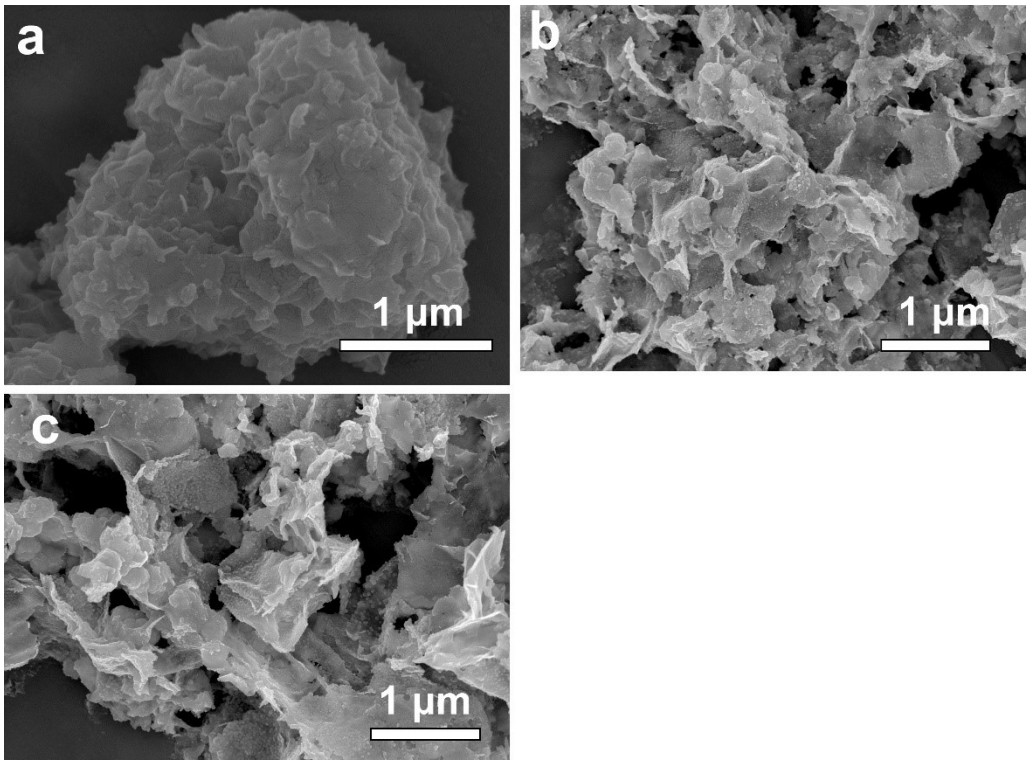

Fig. S4 SEM images of 0.05CdS/N-ZIS (a), 0.1CdS/N-ZIS (b), and 0.15CdS/N-ZIS (c).

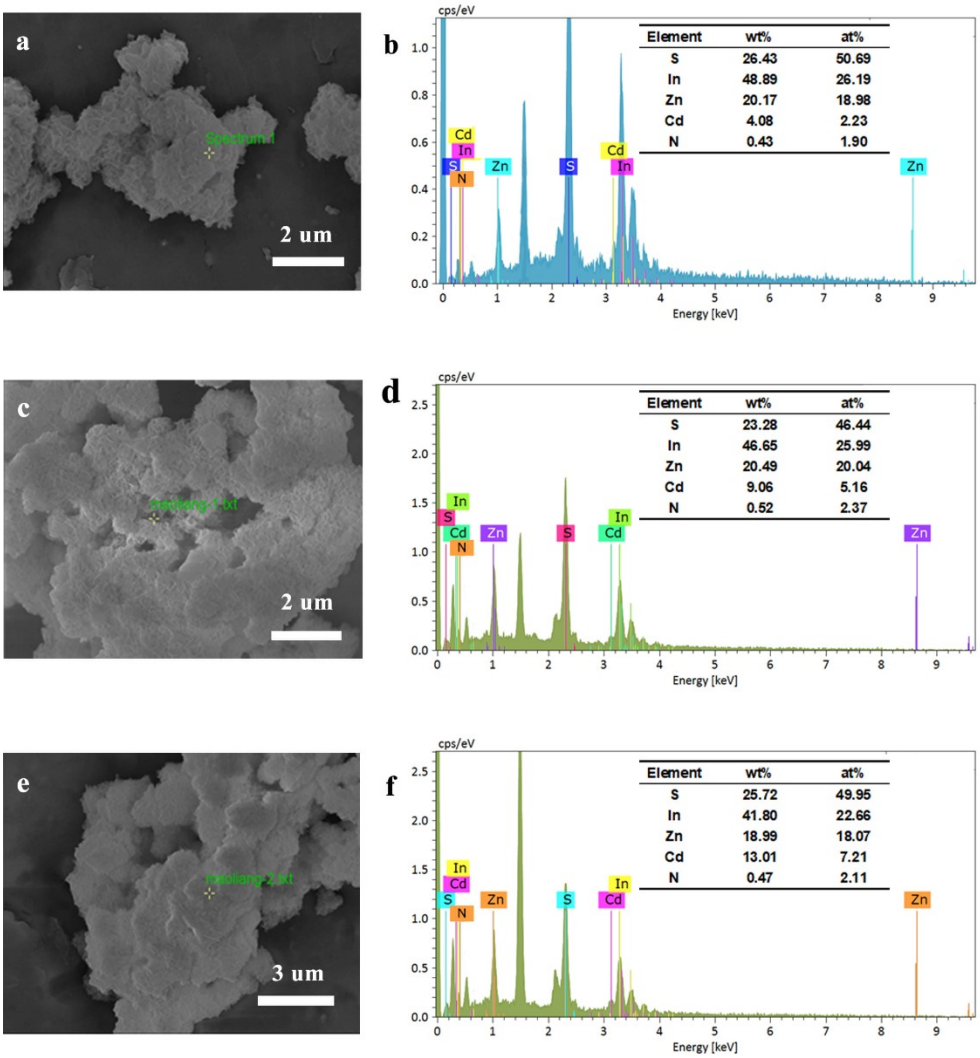

Fig. S5 SEM images (a, c, e) and corresponding EDX spectra (b, d, f) of 0.05CdS/N-ZIS (a, b), 0.1CdS/N-ZIS (c, d), and 0.15CdS/N-ZIS (e, f).

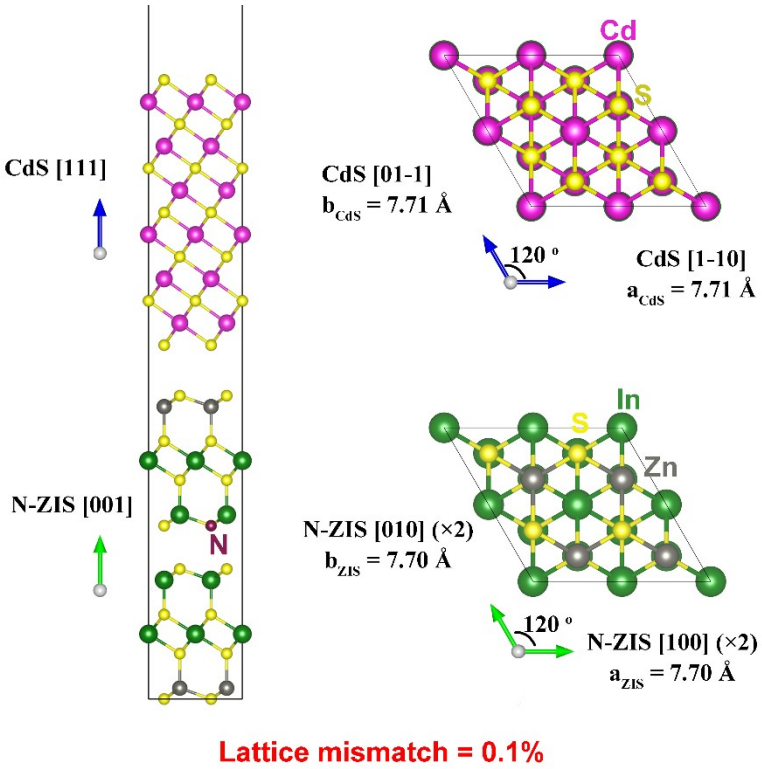

Fig. S6 Model for the interface between CdS(111) and N-ZIS(001) surfaces: side view of CdS/N-ZIS interface (left side), and front view of CdS and N-ZIS layer of CdS/N-ZIS (right side).

The high interface lattice match is essential to form a stable heterostructure, which can be investigated by examining the surface geometry structure of the CdS and N doped ZIS phases. On the basis of the HRTEM analysis, we consider a model for the interface between CdS(111) and N-ZIS(001) surfaces. For CdS(111) surface, the lattice parameters are $a = b = 0.771$ nm. For N-ZIS(001) surface, the lattice parameters are $a = b = 0.770$ nm . In the CdS/N-ZIS interface model, a 1×1 CdS(111) surface slab is used to match a 2×2 N-ZIS(001) surface slab. As shown in Fig. S4, the optimized lattice compatibility along the [100] direction is one a_{CdS} matching to one $a_{N\text{-}ZIS}$, with the lattice mismatch of $(a_{CdS} - a_{N\text{-}ZIS})/a_{N\text{-}ZIS} = 0.1\%$. The low lattice mismatch indicates the intimate interfacial connection of CdS/N-ZIS system.

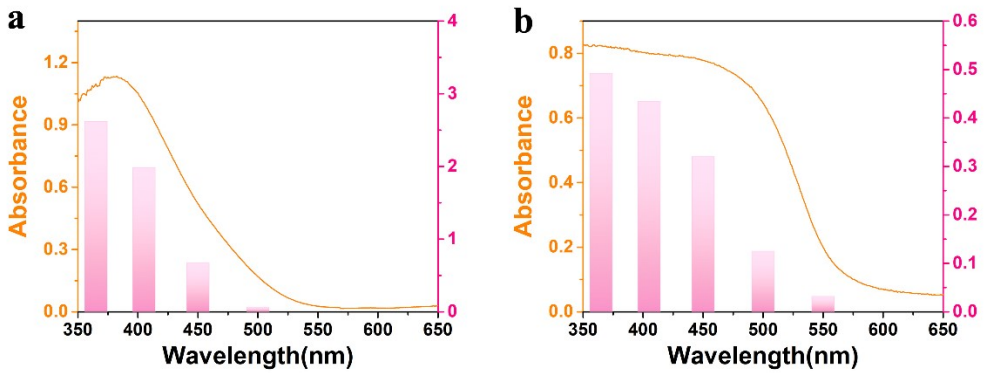

Fig. S7 AQE and UV-vis DRS of N-ZIS (a) and CdS (b).

Table S2. Comparison of representative ZIS-based photocatalysts and their H_2 evolution behaviors.

Catalysts	Condition	H_2 (mmol g^{-1} h^{-1})	AQE
CdS/N-ZIS (this work)	Na_2S-Na_2SO_3 $\lambda > 400$ nm	1.57	8.5% (405 nm)
CeO_2/ZIS [S3]	Na_2S-Na_2SO_3 $\lambda > 420$ nm	0.85	/
N-doped ZIS[20]	TEOA $\lambda > 400$ nm	1.11	~16% (420 nm)
ZIS/Ta_3N_5[S4]	TEOA Simulated solar light	0.83	/
RGO/ZIS[S5]	TEOA (10 vol%) $\lambda > 420$ nm	2.64	4.4% (420 nm)
ZIS/UiO-66[S6]	TEOA (10 vol%) $\lambda > 400$ nm	1.86	1.4% (420 nm)
Ag_xAu_{1-x}/ZIS/TiO_2[S7]	Na_2S-Na_2SO_3 Visible light	0.98	1.47%
rGO/TiO_2/ZIS[S8]	Na_2S-Na_2SO_3 Visible light	0.46	0.69%
ZIS/$In(OH)_3$[S9]	TEOA $\lambda > 420$ nm	1.47	/

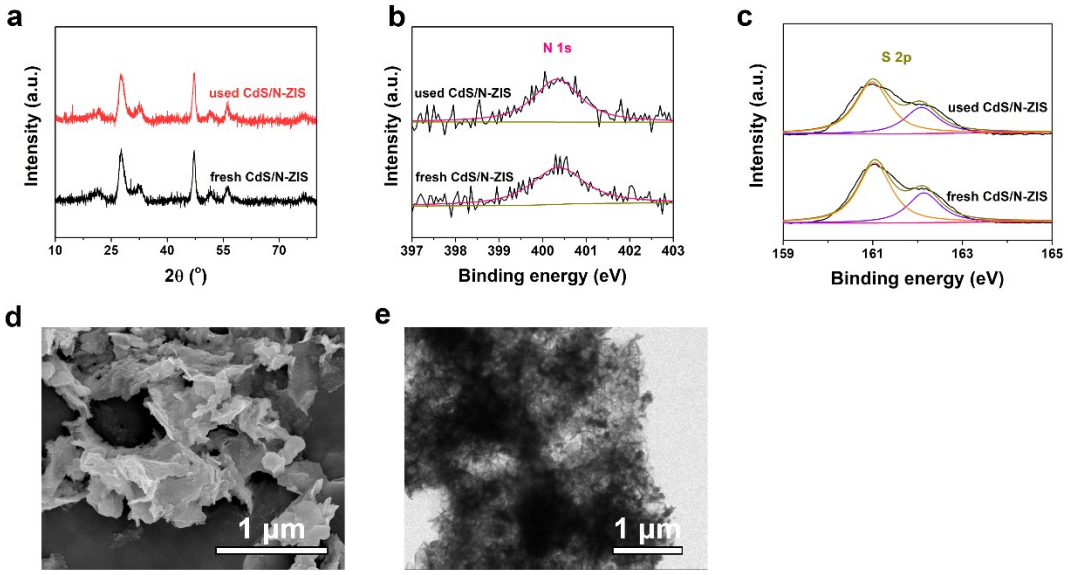

Fig. S8 XRD patterns (a), high resolution XPS of N 1s (b) and S 2p (c) of the fresh and used CdS/N-ZIS sample. SEM (d) and TEM (e) images of the recycled CdS/N-ZIS sample.

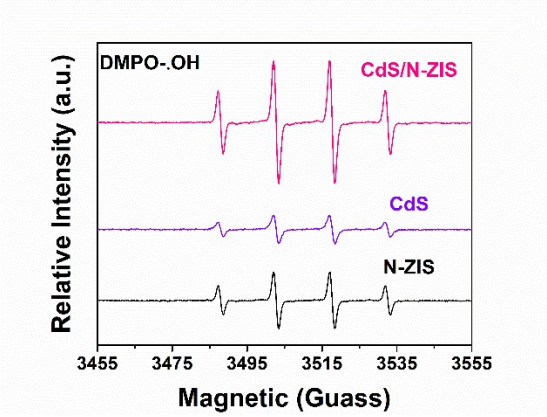

Fig. S9 EPR signals of DMPO-•OH adducts in methanol over various photocatalysts under illumination for 2 min.

Reference

S1. G. Kresse and J. Furthmüller, *Phys. Rev. B*, 1996, **54**, 11169.

S2. G. Kresse and D. Joubert, *Phys. Rev. B*, 1999, **59**, 1758.

S3. M. Zhang, J. Yao, M. Arif, B. Qiu, H. Yin, X. Liu and S.-m. Chen, *Appl. Surf. Sci.*, 2020, **526**, 145749.

S4. Y. Xiao, W. Zhang, Q. Xing, X. Feng, Y. Jiang, Y. Gao, H. Xu, J. Zhang, L. Ni and Z. Liu, *Int. J. Hydrogen Energ.*, 2020, **45**, 30341-30356.

S5. B. Chai, T. Peng, P. Zeng, X. Zhang and X. Liu, *J. Phys. Chem. C*, 2011, **115**, 6149-6155.

S6. J. Jiang, Q. Zhu, Y. Guo, L. Cheng, Y. Lou and J. Chen, *B. Chem. Soc. JPN*, 2019, **92**, 1047-1052.

S7. H. An, H. Wang, J. Huang, M. Li, W. Wang and Z. Yin, *Appl. Surf. Sci.*, 2019, **484**, 1168-1175.

S8. H. An, M. Li, W. Wang, Z. Lv, C. Deng, J. Huang and Z. Yin, *Ceram. Int.*, 2019, **45**, 14976-14982.

S9. Y. Li, Y. Hou, Q. Fu, S. Peng and Y. H. Hu, *Appl. Catal. B: Environ.*, 2017, **206**, 726-733.